Available online at www.sciencedirect.com
ScienceDirect
Journal of Catalysis 254 (2008) 157–169
JOURNAL OF CATALYSIS
www.elsevier.com/locate/jcat

Preparation of carbon supported cobalt by electrostatic adsorption of $[Co(NH_3)_6]Cl_3$

L. D'Souza [a], J.R. Regalbuto [a,*], J.T. Miller [b]

[a] *Department of Chemical Engineering, University of Illinois, MC 110, 810 S. Clinton Street, Chicago, IL 60607 7000, USA*
[b] *BP Research Center, E-1F, 150 W. Warrenville Road, Naperville, IL 60563, USA*

Received 14 September 2007; revised 17 November 2007; accepted 10 December 2007

Available online 5 February 2008

Abstract

Our previous paper [L. D'Souza, L. Jiao, J.R. Regalbuto, J.T. Miller, A.J. Kropf, J. Catal. 248 (2007) 165] presented the synthesis of cobalt catalysts on carbon (Timrex) and silica supports by strong electrostatic adsorption (SEA), using a cobalt hexaamine chloride ($[Co(NH_3)_6]Cl_3$, CoHA) precursor. The CoHA undergoes reductive deammination in an uncontrolled manner in the presence of NaOH and adsorbs as Co_3O_4 on carbon with broad size distribution. The present paper extends these studies toward the end of synthesizing well-dispersed Co oxide particles in a narrow size range on carbon supports using NH_4OH. Cobalt uptake versus pH was determined in NH_4OH and NaOH basified solutions over a number of carbons with varying point of zero charge (PZC). The resulting materials were characterized by ICP, powder XRD, XAS, TPR and STEM. CoHA in the presence of NH_4OH adsorbs as well dispersed as CoO, Co_3O_4 and $Co(OH)_4^{2-}$ depending upon the pH of the adsorption solution. These phases were undetectable by powder XRD and STEM Z-contrast imaging, but could be identified by XAS. Additionally, non-adsorbed CoHA complexes underwent transformation to $[Co(NH_3)_5Cl]Cl_2$ at pH > 11 in solution. After calcinations of 250 °C, particle sizes of Co_3O_4 range from 20–50 Å from NH_4OH and 50–200 Å from NaOH. Maximum metal uptake was approximately 3.3 and 2.7 μmol/m^2 in presence of NaOH and NH_4OH, respectively. The SEA method of preparation was compared with incipient wetness impregnation (IWI) of $Co(NO_3)_2{\cdot}6H_2O$; this method yields Co_3O_4 particles after 250 °C calcinations which are almost as small or in one case, smaller than the calcined SEA samples. Higher metal loadings can be achieved by the SEA method by successive adsorption steps with a little variation in particle size and distribution. However, the main advantage of SEA is in forming mono- or submonolayer of different Co oxide phases on carbon surface.

Keywords: Strong electrostatic adsorption; SEA; Point of zero charge; PZC; $[Co(NH_3)_6]Cl_3$; $[Co(NH_3)_5Cl]Cl_2$; Co_3O_4/C; CoO/C; Co/C; Fischer–Tropsch catalysts; Fuel cell catalysts

1. Introduction

The method of strong electrostatic adsorption (SEA) is a simple, rational method for the preparation of catalysts. Based on the "revised physical adsorption" model [2], it describes the adsorption of metals salts with the oxide support under differing pH of the adsorption solution and is successful in quantitatively predicting the Pt uptake on Al_2O_3 and SiO_2 [3–5] from the $PtCl_6^{2-}$ anion and $Pt(NH_3)_4^{2+}$ cation, respectively. The main consideration for the SEA method is whether support hydroxyl groups protonate or deprotonate at the pH of the impregnating solution. The pH at which the hydroxyl groups are neutral is termed as point of zero charge (PZC). Below this hydroxyl groups protonate and become positively charged and the surface can adsorb anionic metal complex ions such as $[PtCl_6]^{2-}$ and $[Pt(SO_4)_2]^{2-}$. Above the PZC, the hydroxyl groups deprotonate and become negatively charged, and cations such as $[Pt(NH_3)_4]^{2+}$ can strongly adsorb on the surface electrostatically. There exists a pH at which electrostatic force of attraction and hence metal complex adsorption is maximum and the catalysts prepared at that pH, followed by pretreatment, leads to nanoclusters, often between 10–20 Å, with near monodispersity (standard deviation <15% [6]).

There are a number of important applications for Co catalysts including water gas shift (WGS) [7–9], steam reforming of

* Corresponding author. Fax: +1 312 996 0808.
E-mail address: jrr@uic.edu (J.R. Regalbuto).

0021-9517/$ – see front matter
doi:10.1016/j.jcat.2007.12.007

ethanol [10], Fischer–Tropsch [11,12] and methylamines [13] synthesis, and cyclocarbonylation of acetylenes [14]. Mixed cobalt oxide catalysts have also been widely used for the WGS reaction [15–17].

In our earlier work, we reported on Co/C and Co/SiO_2 catalyst synthesis by the SEA method, especially physico-chemical changes of CoHA ($[Co(NH_3)_6]Cl_3$ or hexaammine cobalt chloride) precursor during various preparation steps [1]. In that study, we found that cobalt on carbon particles are large with a broad size distribution and standard deviation. Co_3O_4/carbon catalysts with small particle size and narrow standard deviation is desirable prior to adsorption with noble metal complexes for bimetallic fuel cell catalysts [18]. The main goal of the present work is to find preparation protocol to synthesize small and near monodispersed Co_3O_4/carbon. Small unsupported cobalt particles are easy to produce and good synthetic protocols are known in colloidal chemistry especially by the thermal decomposition of carbonyl complexes [19]. But to date no well established protocols exist to synthesize near monodispersed supported Co oxide or metal nanoclusters (particle sizes between 10–100 Å [20]) from aqueous solutions with readily available metal salts. In the current work, it is shown that through control of the preparation variables, small cobat oxide particles can readily be prepared on a variety of carbon supports.

2. Experimental

2.1. Chemicals

$[Co(NH_3)_6]Cl_3$ (CoHA), $Co(NO_3)_2{\cdot}6H_2O$ and CoO (product No. 343153, −325 mesh, average particle size <10 μm) and Co_3O_4 (product No. 203114, 99.995%) were obtained from Aldrich. Commercially available carbons were obtained from the manufacturers. Their designation, surface area and points of zero charge are given in Table 1. KB-600, KB-300, BP and VXC are carbon blacks obtained by pyrolysis of natural gas or oil fraction from petroleum processing [21]. AS is natural graphite and TX is graphite produced from petroleum coke [22]. KBB and CA are activated carbons obtained through chemical activation from coconut shells, wood, peat or coal [23]. High surface area Co_3O_4 (BET surface area 38 m^2/g) was prepared from $Co(CO_3)_2$ and supplied by UOP, Des Plaines, IL.

Table 1
Physical characteristics of different carbons

Carbon source	Abbreviation	Surface area (m^2/g)	Pore vol. (ml/g)	PZC
Norit CA-1, NC 99006, Norit Americas Inc., USA	CA	1400	1.7	2.6
Timrex 04088 N754, Timcal graphite and carbon, Switzerland	TX	280	1.0	4.5
Darco KB-B, Norit Americas Inc., USA	KBB	1500	4.0	4.8
Asbury grade 4827, The Asbury Graphite Mills, Inc., USA	AS	115		5.2
Keitzen black EC 600JD, Akzo Nobel, USA	KB	1250	9.0	9.4
Vulcan XC 72, GP-3845, Cabot Corporation, USA	VXC	254	2.0	8.9
Black pearls 2000, Cabot Corporation, USA	BP	1475	7.1	9.5

2.2. Catalyst preparation

The equilibrium adsorption uptake of CoHA onto carbon was determined as a function of pH, from solutions of constant metal concentration. Adsorption experiments were conducted with an excess of liquid to prevent large shifts in the solution pH due to the oxide buffering effect [24]. The surface loading is the amount of support surface area per liter of adsorption solution. For example, 0.1 g of 250 m^2/g carbon in 50 ml of solution yields a surface loading of 500 m^2/L, or about a 500-fold excess of the TX pore volume. The 50 ml polypropylene bottles containing 200 ppm CoHA solutions and support were shaken for 1 h, after which 3–4 ml filtered solution was analyzed by inductively coupled plasma (ICP) for Co remaining in the solution. The cobalt uptake was determined as the difference in Co concentrations in the initial and post-contacted solutions. The pH was adjusted with HCl, HNO_3, NH_4OH and NaOH. The error in ICP measurement is ±5%.

Larger samples (1 g) of catalysts were prepared at the pH of maximum uptake, which corresponds to optimal condition for strong electrostatic adsorption. The filtered solids were air-dried overnight and calcined at 200–250 °C in a muffle furnace for 1 h.

Cobalt catalysts were also prepared by IWI method using CoHA or $Co(NO_3)_2{\cdot}6H_2O$. Several portions of this highly concentrated solution were added to the carbon supports with frequent mixing of the wet powder. The slurry was dried at room temperature for 24 h, followed by drying in oven at 100 °C for 12 h and finally calcined at 250 °C for 1 h.

2.3. Characterization

Powder X-ray diffraction analyses were performed using a Siemens D5000 diffractometer with Cu$K\alpha$ radiation (λ = 1.5406 Å) operating at 30 kV and 40 mA, operating in Bragg–Brentano geometry. A 'locked coupled' scan mode in the 20–70° 2θ range, step size of 0.01° and 2.5 s exposure for each point were used.

UV–visible spectra were recorded at a scan rate of 100 nm min^{-1} using Perkin–Elmer spectrometer with Win Lab 5.1.4.0630 software.

Barrett–Johner–Halenda 'BJH' adsorption average pore width was calculated from N_2 adsorption experiment using Surface area and porosity analyzer, supplied by Micromeritics, model ASAP 2020.

Temperature programmed reduction (50 ml/min 10% H_2 in Ar and 50 mg of sample) and desorption (50 ml/min 100% Ar) (TPR and TPD, respectively) were conducted using AutoChem II instrument supplied by Micromeritics. A ramp rate of 10 °C/min was used in all experiments. No special gases were adsorbed prior to the TPD experiment, rather evolution of

any adsorbed gases at ambient conditions, or decomposition of functional groups was tested.

Scanning transmission electron microscopic (STEM) analyses of the catalysts were obtained by adding isopropanol and sonicating this slurry for 5 min. Samples were placed onto a carbon-coated copper grid. STEM and EDX experiments were obtained using a JEOL electron microscope (JEM-2010F FasTEM FEI) operating at 200 kV and an extracting voltage of 4500 V. The copper grid (200 mesh, Cu PK/100) was supplied by SPI supplies, USA. Around 1000 particles were analyzed for the size distribution calculation. The number weighted mean particle size (x_N) was calculated using $\sum fx/\sum f$ and standard deviation was calculated using $\sqrt{\frac{\sum f(x-x_N)^2}{\sum f}}$, where x is diameter of the particle, x_N is number weighted mean particle size and f is frequency of occurrence. The surface area weighted mean particle size (x_A) was calculated using $[\sqrt{\sum(\frac{f}{\sum f})(\frac{x}{2})^2}]\times 2$ and the standard deviation was calculated using $\sqrt{\frac{\sum f(x-x_A)^2}{\sum f}}$. Number weighted mean particle size (x_N) and standard deviation have been used in most places unless otherwise stated.

X-ray absorption spectroscopy (XAS) measurements were performed at the advanced photon source (APS) at Argonne National Laboratory (Argonne, IL) on the undulator beamline of the Materials Research Collaborative Access Team (MR-CAT). Details of the EXAFS data collection and analysis are given in previous papers [25]. The data was collected purely in transmission on catalyst samples pressed into thin disks inside of a 6-sample holder. The catalysts transferred into a tubular reactor with Kapton windows and reduced at 450 °C for 1 h in flowing 4% H_2/He. Standard procedures were used to fit the XAS data with WinXAS 97, Version 1.0 software. $[Co(NH_3)_6]Cl_3$, Co foil, CoO, $Co(NO_3)_2{\cdot}6H_2O$ and Co_3O_4 were used as XANES standards. $[Co(NH_3)_6]Cl_3$ and Co foil were used as Co–N ($N_{Co-N} = 6$, $R = 1.97$ Å) and Co–Co ($N_{Co-Co} = 12$, $R = 2.55$ Å) EXAFS references, respectively. The results were generally accurate to ±10% in coordination number. The first shell fits were done in R-space of the k^2-weighted data from 2.7–12.2 $Å^{-1}$.

3. Results

The PZC of carbons used in the present study range from 2.5 to 9.5; values are given in Table 1. The PZC's are measured by EpHL experiments [24] and details will be given else where [26]. Fig. 1a shows the effect of the support on the solution pH shift in control experiments (no added Co) for the different carbons viz. TX, AS, VXC, CA and high surface area Co_3O_4. The acidic–basic properties of the support hydroxyl groups buffer the solution pH leading to a plateau in the figure [25]. The pH_{final} plateaus for TX, AS, VXC, CA and high surface area Co_3O_4 lies around 5, 5, 7, 3 and 9, respectively, showing system is approaching PZC of the respective carbons. Usually, system will approach to PZC of the oxide between 60,000 to 100,000 m^2/L surface loading. Figs. 1b, 1c, 1d and 1e give pH shifts and metal uptake results from the CoHA adsorption experiments. At pH's below about 3, there is little Co adsorption and the pH shift curves are similar to the Co-free solutions; however, for above a pH of about 4, the pH plateau of TX, AS and VXC increased from 3 and 5 to about 9, close to the PZC of pure Co_3O_4, Figs. 1b and 1c. For CA carbon, the pH_{final} plateau increases slightly to around 4 with the CoHA solution, however, little Co is adsorbed up to a pH of about 9, thus this is only slightly different from that of the support.

The CoHA uptake for carbons is given in Figs. 1d and 1e for NaOH and NH_4OH, respectively. The uptake of this complex cation takes place in basic pH as proposed in the previous work [27]. For all carbons, little CoHA is adsorbed below a pH of about 8, but increases rapidly with increasing pH. In NaOH, Co uptake increases rapidly at pH larger than 9. CoHA solutions at pH above 9 were stable with no precipitates formed. After the maximum uptake at pH of about 10 in NH_4OH, there occur sharp decreases in the amount of Co adsorbed on each carbon. In presence of NaOH, there is a higher uptake of Co than for NH_4OH solutions and the maximum in adsorption occurs at a pH > 11 versus 10. The maximum uptake values for TX, AS, CA and VXC are 3.7 (pH 11.5), 3.3 (pH 13), 3.4 (pH 13.2), 3.5 μmol/m^2 (pH 13.1) in the presence of NaOH and 2.5 (pH 10.1), 2.3 (pH 10.1), 0.9 (pH 10.4) and 2.7 (pH 10.0) μmol/m^2 in the presence of NH_4OH, respectively. These are similar for each case (NaOH and NH_4OH), with the exception of CA carbon. This activated carbon has the highest surface area and smallest pore sizes of the set. In a previous paper, cationic platinum complexes were shown to be excluded from a significant fraction of the pore volume of high surface area carbons, since they retain more hydration sheath than do anionic complexes [27]. Exclusion from small pores is thought to occur here with the cobalt amine cation. Another striking feature in Figs. 1d and 1e is that the Vulcan, with a PZC of 8.9 (Table 1) adsorbs Co to the same extent as the other carbons which all have much lower PZCs.

Above a pH of 12 with NH_4OH, little CoHA is adsorbed on any carbon. UV–visible spectroscopy of CoHA and CoHA with TX carbon at pH initial of 12 is shown in Fig. 2. There was a significant shift to higher wavelength, which takes nearly 4 h to complete, for the CoHA solution. The final pH of the adsorption solution was 11.6. Thus, while little Co adsorbs, the CoHA complex in solution undergoes some change in the presence of carbon support, while in the absence of the carbon support there is no change in the spectra. The shift in the wavelength from 476 to 504 nm indicates that the transformation is complete in about 4 h. Pure $Co(NH_3)_6Cl_3$ solution is orange in color and this color does not change even for 6 months. The transformed Co complex solution was pinkish in color and it can be easily observed with naked eyes or UV–visible spectroscopy. Color change is a direct evidence for ligand transformation in the $Co(NH_3)_6Cl_3$.

3.1. Molecular state of adsorbed CoHA on carbon

The composition of the adsorbed Co species on TX carbon was examined by XANES and EXAFS at four different pHs by

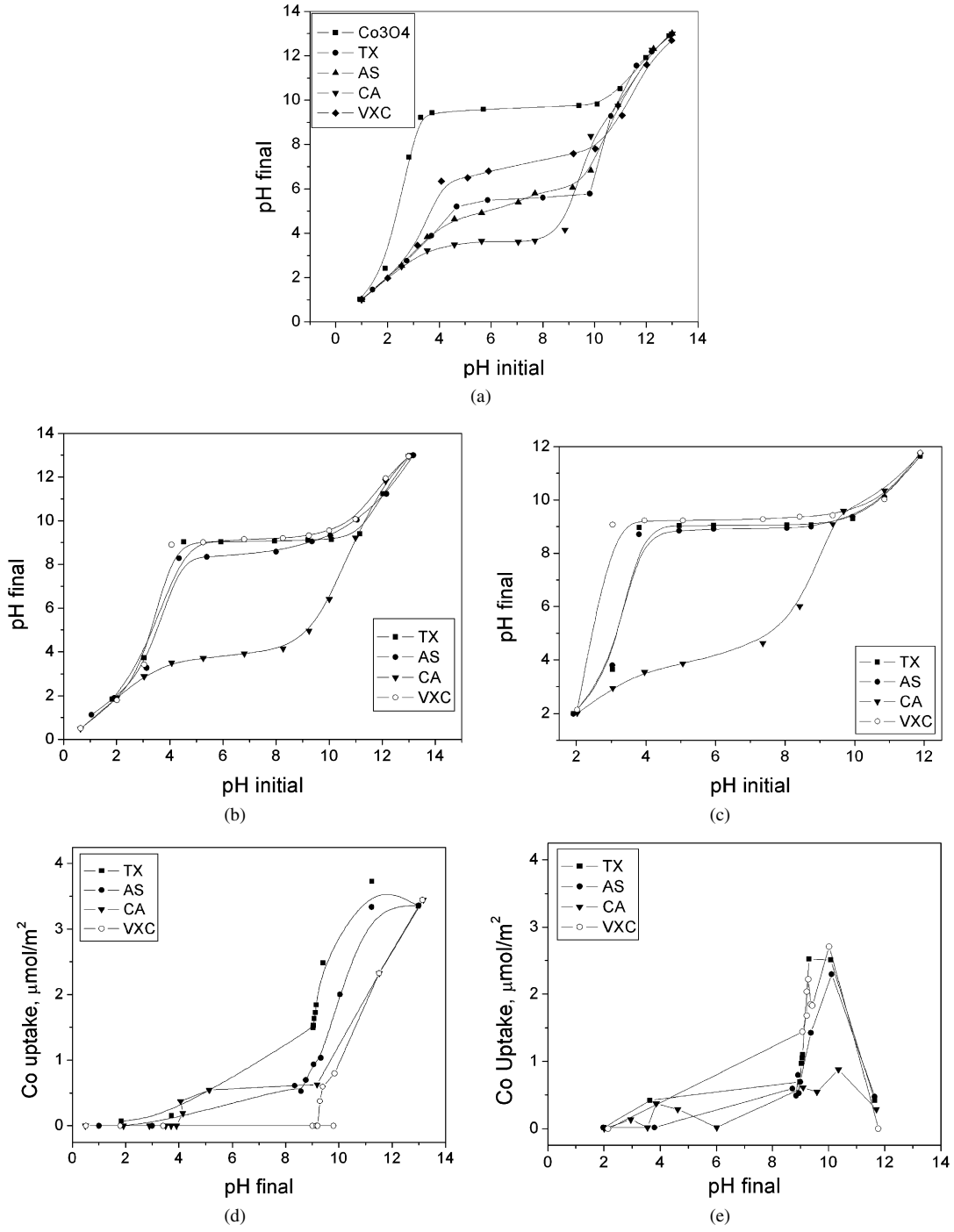

Fig. 1. (a) pH shift with pure materials–control experiment; CoHA solution pH shifts for different carbons (∼200 ppm CoHA, 1000 m^2/L), (b) when NaOH and HCl and (c) when NH_4OH and HCl were used to adjust the pH; Co^{3+} uptake on different carbons versus pH, (d) when NaOH and HCl and (e) when NH_4OH and HCl were used to adjust the pH. The error in metal uptake is ±5%.

the addition of NH_4OH. The initial solution pH was ∼7 (natural pH of 200 ppm CoHA), 10.8, 11.6 and 12.5. The final pH's of impregnating solution were 9.2, 9.8, 11.2 and 12.3, respectively, and powder X-ray diffraction patterns showed no crystalline peaks on any CoHA/TX and dried catalyst confirming the species are molecularly adsorbed, or highly disordered. Fig. 3 gives the XANES of the reference compounds $[Co(NH_3)_6]Cl_3$ and $Co(NO_3)_2{\cdot}6H_2O$ and the EXAFS fits are given in Table 2. $Co(NO_3)_2$ has 6 Co–O bonds at 2.05 Å, while there are 6 Co–N bonds at 1.96 Å for $[Co(NH_3)_6]Cl_3$. The EXAFS analysis of bulk CoO and Co_3O_4 are also given in Table 2. The CoO has 6 Co–O bonds at 2.13 Å, while Co_3O_4 has 5 Co–O neighbors at 1.92 Å, i.e., 50% Co^{2+} with 4 Co–O at 1.94 Å and 50% Co^{3+} at 1.92 Å. EXAFS cannot distinguish between Co–O and Co–N scatters, however, these atoms can be identified by the differences in bond distance and Co–O–Co distance in the higher shell. The first shell fits of EXAFS for CoHA/TX at different pH are also summarized in Table 2 and XANES spectra are

shown in Fig. 4. At each pH, the XANES spectra are significantly different from that of CoHA indicating there has been a significant change in the Co species upon adsorption. At final pH of 9.2, i.e., without any added NH_4OH, CoHA undergoes reduction to Co^{2+} with the formation of CoO ($N_{Co–O} = 6.0$ at 2.08 Å and $N_{Co–O–Co} = 4.9$ at 3.10 Å). At final pH of 9.8, with addition of some NH_4OH, CoHA is converted to Co_3O_4 with $N_{Co–O} = 4.7$ at 1.92 Å and $N_{Co–O–Co} = 3.2$ at 2.83 Å, while at higher pH (11.2 and 12.3) with more NH_4OH CoHA is reduced to Co^{2+} with 4 Co–O ligands at 2.01 Å. At the pH 11.2 and 12.3, the XANES shape is consistent with oxygen ligands although the exact structure cannot be positively identified. The

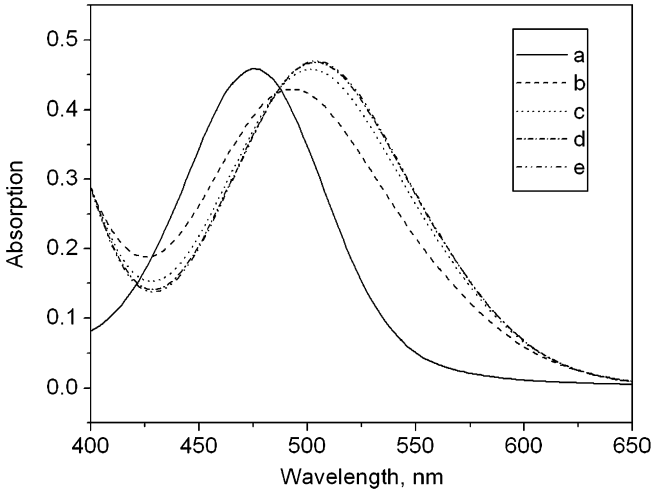

Fig. 2. UV–visible spectrum of CoHA solution at $pH_{initial}$ 12 (pH_{final} 11.6) in contact with TX carbon (NH_4OH and HCl were used to adjust the pH). Spectrum a was for pure 500 ppm CoHA solution, b, c, d and e are for same solution after contacting with TX at 1, 2, 3 and 4 h (final pH of the contacting solution was 11.6). No change in the initial spectra was observed in the absence of TX carbon.

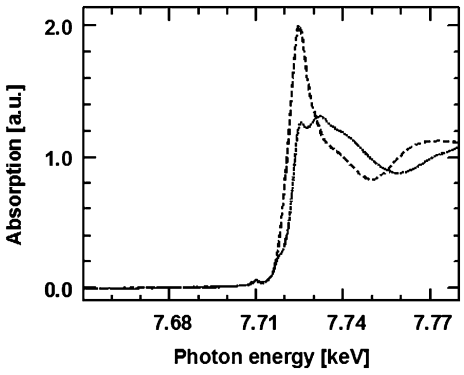

Fig. 3. XANES of reference compounds; bulk $Co(NO_3)_2 \cdot 6H_2O$ (dash) and bulk CoHA (dot). Compounds are diluted with amorphous silica for XAS measurements.

Table 2
Co EXAFS fits for reference compounds and cobalt species adsorbed on TX at different pH's (k^2: Δk2.75–12.2^{-1} Å) with NH_4OH

Catalyst	Final pH	Structure of adsorbed Co	Backscatter	CN	R (Å)	DWF ($\times 10^3$)	Eo (eV)
			References				
$Co(NO_3)_2 \cdot 6H_2O$			Co–O	6.0	2.05	−2.8	−5.3
$Co(NH_3)_6^{3+}$			Co–N	6.3	1.96	0.0	0.6
CoO			Co–O	6	2.13		
			Co–O–Co	12	3.02		
Co_3O_4			50% C–O	6	1.92		
			50% C–O	4	1.94		
			CO–O–Co	6	2.86		
			Carbon, dried at room temperature				
CoHA/TX	SEA	Similar to CoO	Co–O	6.0	2.08	4.0	0.2
(XANES = 1.0 CoO)	pH 9.2		Co–O–Co	4.9	3.10	0.5	2.4
CoHA/TX	SEA	Similar to Co_3O_4	Co–O	4.7	1.92	0.5	−6.1
	pH 9.8		Co–O–Co	3.2	2.83	−0.5	−3.1
CoHA/TX	SEA	$Co(OH)_4^{2-}$	Co–O	4.2	2.01	−0.5	−5.5
	pH 11.2						
CoHA/TX	SEA	$Co(OH)_4^{2-}$	Co–O	4.2	2.04	−0.5	−4.3
	pH 12.3						
Non-adsorbed Co (solution Co)	pH > 11	$Co(NH_3)_5Cl^{2-}$	Co–N	5.1	1.96	−2.7	1.5
			Co–Cl	0.9	2.26	−2.7	−5.6
			Carbon, reduced at 450 °C				
CoHA/TX	SEA	Metallic Co	Co–Co	8.9	2.51	0.0	−1.9
	pH 9.8						
CoHA/TX	SEA	CoO	Co–O	3.0	2.10	4.0	−3.1
(XANES: 0.45 Co^0 + 0.55 CoO)	pH 11.2						
		Co–O–Co	4	3.05	0.5	2.0	
		Metallic Co	Co–Co	4.1	2.50	2.0	−2.6
CoHA/TX	SEA	CoO	Co–O	2.9	2.10	1.0	0.0
(XANES: 0.45 Co^0 + 0.55 CoO)	pH 12.3						
			Co–O–Co	4.2	3.02	0.5	−0.8
		Metallic Co	Co–Co	3.3	2.51	0.0	−0.4

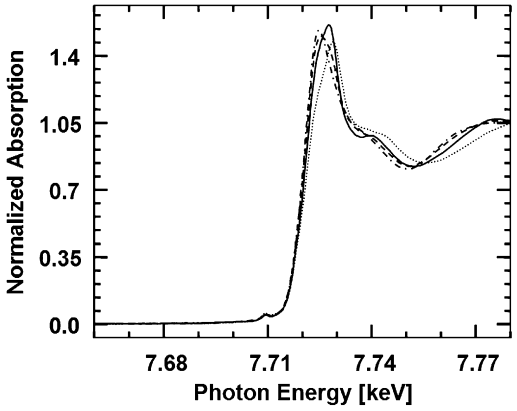

Fig. 4. XANES of CoHA adsorbed on TX at pH_{final} 9.2 (solid), pH_{final} 9.8 (dot), pH_{final} 11.2 (dash) and pH_{final} 12.3 (dash dot) (NH_4OH and HCl were used to adjust the pH). The XANES's spectra indicate a change in structure of CoHA upon adsorption, and the structures differ at each pH.

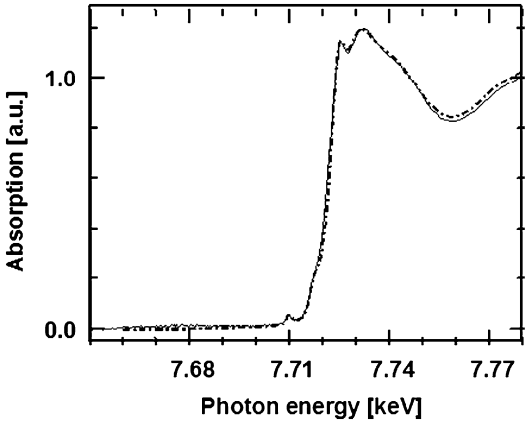

Fig. 5. XANES of $[Co(NH_3)_6]Cl_3$ (dash dot) and non-absorbed Co species (solid) at pH_{final} 11.6. (NH_4OH and HCl were used to adjust the pH). The XANES indicate that the initial CoHA and non-adsorbed Co have very similar oxidation state and structure, i.e., Co^{3+} with NH_3 ligands.

bond distance is consistent with that in $Co(NO_3)_2{\cdot}6H_2O$, although the ligands could be hydroxide or aquo ligands. There are no higher shells, i.e., Co–O–Co in the EXAFS. In addition, at the high OH^- concentration the likely ligands are OH^- and not H_2O ligand.

Table 2 also gives the structure of the cobalt species after reduction at 450 °C. Cobalt on carbon adsorbed at a final pH of 9.8, i.e., Co_3O_4 undergoes complete reduction Co metal with $N_{Co–Co} = 8.9$ at a distance of 2.51 Å. The coordination number is consistent with moderately sized metallic particles of about 50 Å [28]. Reduction of cobalt on carbon prepared at pH_{final} of 11.2 is only partially reduced by H_2 at 450 °C to Co metal with $N_{Co–Co} = 4.1$ at a distance of 2.50 Å. The fit of the Co–O peak ($N_{Co–O} = 3.0$ at 2.10 Å) and the position of the Co–O–Co ($N_{Co–O–Co} = 4$ at 3.05 Å) suggest that CoO has also formed. A fit of XANES spectra indicates that about 45% of the Co is metallic with 55% unreduced CoO. Since only a portion of the Co is reduced, the true coordination number is given by the fit value divided by the fraction of the metallic cobalt (e.g., $4.1/0.45 = 9.1$), indicating the formation of moderate sized metallic particles [28]. The sample prepared at pH_{final} 12.3 exhibited similar characteristics like that prepared at pH_{final} 11.2 with the coordination of metallic Co particles $3.3/0.45 = 7.3$, indicating smaller particles have formed. The overall reduction trend of different species indicates that Co_3O_4/C is more easily reducible than $Co(OH)_4^{2-}$/C or CoO/C. This is consistent with the previous study on carbon and silica where only adsorbed Co_3O_4 adsorbed cobalt is fully reduced to metallic Co [1].

Fig. 5 gives the XANES of the reference compound CoHA as well as the non-adsorbed cobalt species remaining in solution at final pH of 11.6 (product extracted by drying the solution at ambient conditions used for adsorption experiment†). The similarity of the two spectra is consistent with no change in the oxidation state, i.e., Co^{3+} and still containing several NH_3 ligands. The first shell coordination is consistent with 5 Co–NH_3 bonds ($N_{Co–N} = 5.1$) at 1.96 Å and one Co–Cl bond ($N_{Co–Cl} = 0.9$) at 2.26 Å (Table 2). EXAFS and XANES are consistent with the structure of non-adsorbed cobalt species as $[Co(NH_3)_5Cl]Cl_2$. Powder XRD studies confirms this assignment. The XRD patterns for the bulk CoHA and the non-adsorbed cobalt species† at pH_{final} 11.6 are shown in Fig. 6. The diffraction pattern of non-adsorbed cobalt exactly matches a mixture of $[Co(NH_3)_5Cl]Cl_2$ (PDF No. 01-0180, main peaks $2\theta = 15.5, 21.7, 22.6, 27$) and NH_4Cl (PDF No. 34-0710, main peaks $2\theta = 22.9, 32.5, 47$). At a pH_{final} of 11.6, the EXAFS indicates that the non-adsorbed Co remains in a Co^{3+} oxidation state (Fig. 5), although its structure is changed, but the adsorbed species are in the Co^{2+} oxidation state (Fig. 4).

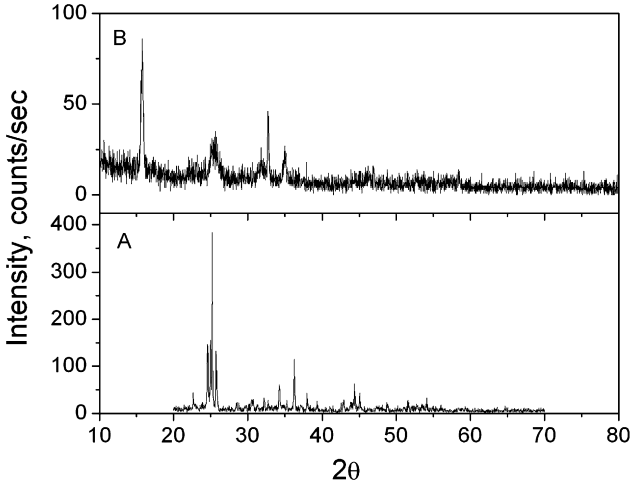

Fig. 6. Powder X-ray diffraction of (A) bulk CoHA and (B) unadsorbed cobalt at pH_{final} 11.6 (product extracted by drying the solution used for adsorption experiment; NH_4OH and HCl were used to adjust the pH).

TPR profiles for CoHA/TX samples prepared at different final pH (pH adjusted with NH_4OH) are shown in Fig. 7A. TPR of pure TX as well as pure CoO and Co_3O_4 are also shown for reference. The peak position of maximum H_2 consumption and their assignments are given in Table 3. While TPD of TX in Ar (Fig. 7A-h) does not show any gas evolution up to 800 °C, the TPR profile of TX (Fig. 7A-e) shows continuous consumption of H_2 with a maximum at 570 °C, most probably due to formation of CH_4 by gasification of carbon [29]. Reduction of CoO (Fig. 7A-g) shows a maximum in H_2 consumption

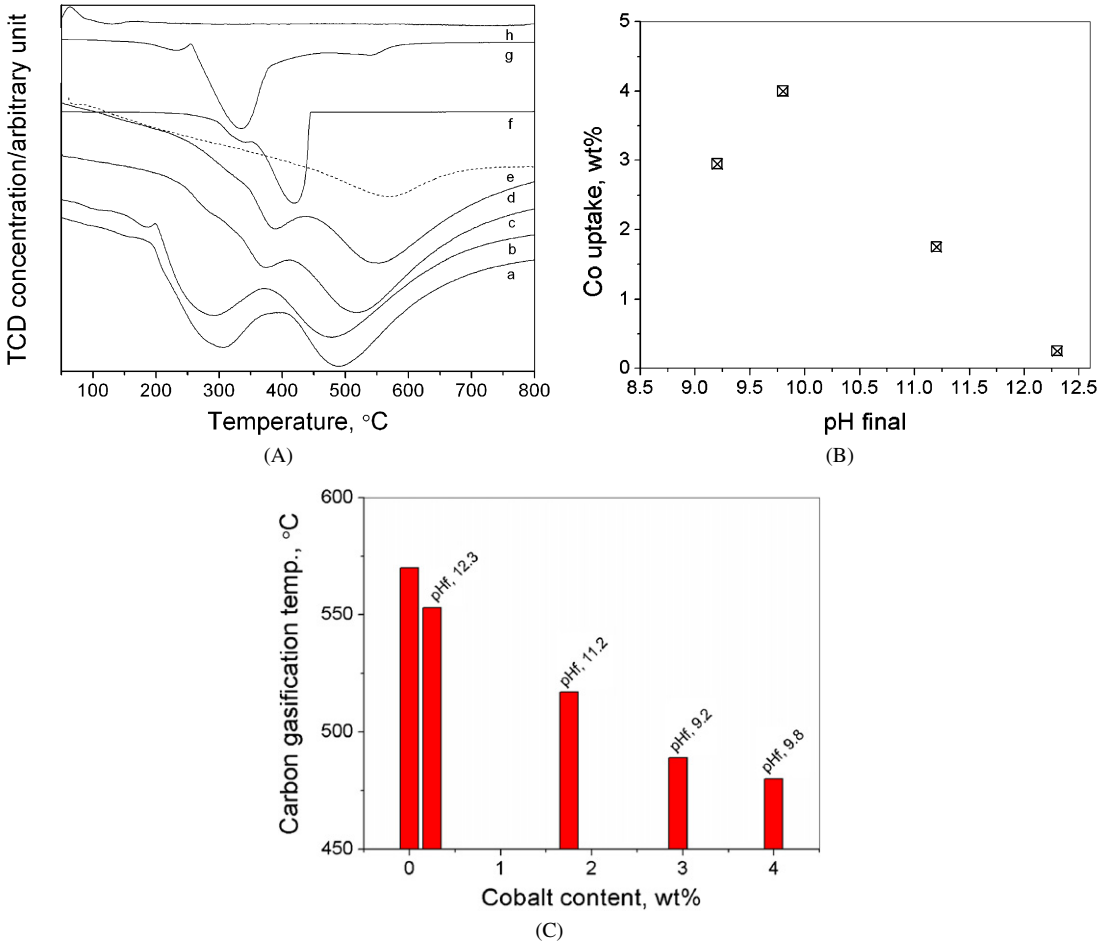

Fig. 7. (A) TPR of CoHA/TX at different pH_{final} (a) 9.2, (b) 9.8, (c) 11.2 and (d) 12.3. (e), (f) and (g) are TPR of TX carbon support, Co_3O_4 and CoO, respectively, and (h) TPD of TX carbon support; (B) Co uptake on TX carbon at different pH and (C) carbon gasification temperature vs cobalt content in the catalysts.

Table 3
TPR peaks position and their assignments

Sample	Peak position, reduction temp. (°C)	Assignment
TX	570	Gasification
Pure Co_3O_4	340	$Co^{3+} \rightarrow Co^{2+}$
	420	$Co^{2+} \rightarrow Co$
Pure CoO	230	$Co^{3+} \rightarrow Co^{2+}$
	333	$Co^{2+} \rightarrow Co$
CoHA/TX, pHf 9.2	302	$Co^{2+} \rightarrow Co$
	489	Gasification
CoHA/TX, pHf 9.8	185	$Co^{3+} \rightarrow Co^{2+}$
	290	$Co^{2+} \rightarrow Co$
	480	Gasification
CoHA/TX, pHf 11.2	380	$Co(OH)_4^{2-}$ to Co
	517	Gasification
CoHA/TX, pHf 12.3	380	$Co(OH)_4^{2-}$ to Co
	553	Gasification

at 333 °C, due to the reduction of Co^{2+} to Co. There is also a small shoulder around 230 °C, which may be due to the reduction of contaminant Co^{3+} compounds, perhaps Co_3O_4, to Co^{2+}. The Co_3O_4 TPR profile (Fig. 7A-f) shows a two-step reduction with maxima around 340 °C (Co^{3+} to Co^{2+}) and reduction of Co^{2+} to Co at 420 °C. These trends are consistent with previous reports by Noronha et al. [30] and van Steen et al. [31]. In study by Noronha [30], the Co^{2+} to Co reduction occurred around 415 °C, while van Steen et al. [31] reported metallic reduction at about 315 °C. The difference in reduction temperatures is may be due to different oxide particle size, gas flow rate and heating ramp.

The TPR profile of CoHA/TX prepared at different final pH's by the addition of NH_4OH shows that the maximum reduction temperature (due to gasification of the carbon support) decreases with increasing Co content. Fig. 7B gives the relative Co content in different samples. As the amount of Co on the carbon increases, the temperature of the gasification peak (highest reduction peak) decreases from 570 to 553 °C (Fig. 7A-d) for sample prepared at pH_{final} of 12.3, followed by sample prepared at pH 11.2 showing a peak at 517 °C (Fig. 7A-c), pH_{final} 9.2 showing a peak at 489 °C (Fig. 7A-a), and pH 9.8 showing a peak at 480 °C (Fig. 7A-b). Fig. 7C summarized the above results.

The sample prepared at pH 9.2 (Fig. 7A-a, which contains only CoO species adsorbed on TX, shows a peak at 302 °C corresponding to the reduction of Co^{2+} to Co. A sample prepared at pH 9.8 (Fig. 7A-b) which contains Co_3O_4 species adsorbed on TX, shows a small peak at 185 °C corresponding to the reduction of Co^{3+} to Co^{2+} and a decent peak at 290 °C cor-

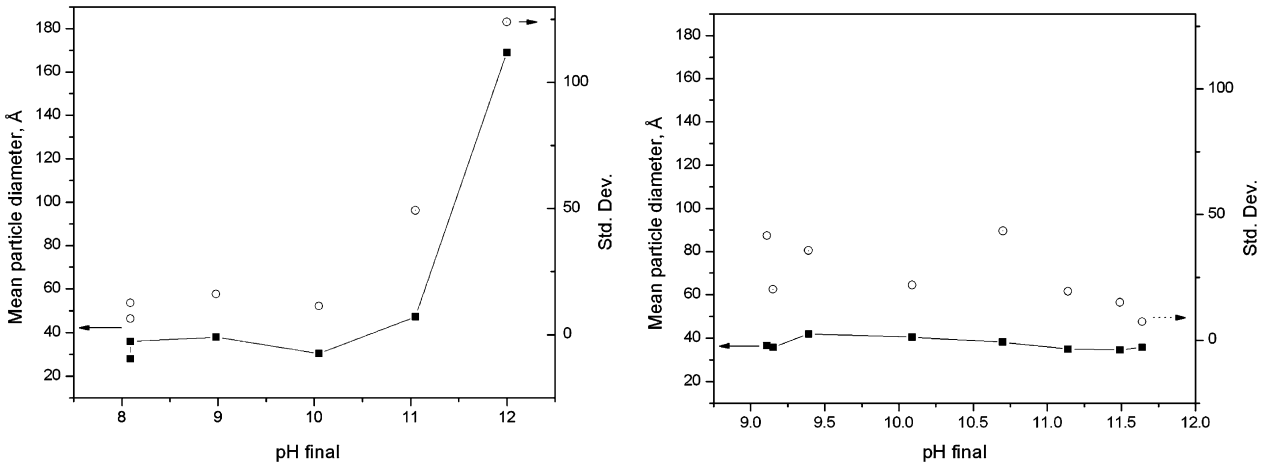

Fig. 8. Statistical mean particle diameter and standard deviation for Co_3O_4 nanoparticles supported on carbon (TX) after calcination at 250 °C. Effect of NaOH (left) and NH_4OH (right). Solid line and solid squares correspond to particle diameter; and open circles correspond to standard deviation.

responding to reduction of Co^{2+} to Co. Samples prepared at pH 11.2 and 12.3 (Figs. 7A-c and 7A-d) show a reduction peak at 375 and 380 °C, respectively, corresponding to the reduction of $Co(OH)_4^{2-}$ to Co. These results have been summarized in Table 3.

The particle size distribution of Co oxide particles prepared by SEA on TX carbon at different pHs in presence of NaOH and NH_4OH were analyzed by STEM z-contrast imaging and Powder XRD. For no NaOH or NH_4OH basified sample could any oxide particles be imaged in the dried state. Furthermore, there did not appear any large patches of amorphous cobalt-containing phases. In addition to that, no diffraction peaks are seen in powder XRD experiments. It appears from STEM that the Co oxides formed upon adsorption with carbon in ammonia-basified solutions are monolayer dispersed which, upon calcination form nanometer sized particles but larger amorphous Co_3O_4 particles form upon adsorption from NaOH solutions [1] which upon calcination become more crystalline and STEM identifiable.

Cobalt oxide particles formed from NH_4OH-basified adsorption solution upon calcination at 250 °C; these are shown in Fig. 8 and are compared to NaOH-basified samples calcined at the same temperature. Distributions in both cases are similar below pH 11 with an average particle size about 30–50 Å. Above a pH of 12 with NaOH, the mean particle size increases to over 150 Å with a large standard deviation, whereas with NH_4OH, they remain small ≈40 Å. On the other hand, in the presence of NH_4OH, with the increase in pH the mean particle size remains nearly constant or decreases slightly. STEM images of cobalt oxide particles on TA and AS are shown in Figs. 9a and 9b, respectively. Although the metal loadings and support PZC's are similar, the oxide particles on AS carbon are smaller than that on TX carbon (Figs. 9c and 9d). Fig. 9d also gives particle size distribution with different duration of calcination. Calcination at 250 °C for 1 h resulted in particles about 27 Å, which increased to 33 Å after calcining for 5 h. Thus, the calcination temperature and duration have also have a significant effect on the cobalt oxide particle size, although this step in the preparation has not be optimized.

STEM also showed that below an initial pH 9.00, the particles loosely adhere to carbon surface. These particles are easily removed from the surface by sonication. These results suggest that the cobalt species adsorbed below a pH of about 9 (see Fig. 1e) are not strongly adsorbed on the support, i.e., not SEA.

One of the limitations of the SEA synthesis method is a limit in the metal loading. Since the support can adsorb up to a maximum of one monolayer of the metal complex, the surface area of the support and the geometric size of the adsorbed (hydrated) metal complex limit the loading. However, by successive adsorption, with calcination between adsorptions, the metal loading can be increased. Multiple adsorption of CoHA was conducted on TX carbon at an initial pH equal to 11.3. After each adsorption, the catalyst was washed with deionized water and calcined at 250 °C for 1 h. The metal loading increased from 1.6 to 5.6 wt% after three successive adsorptions. With subsequent adsorptions, the metal loading increased, however cobalt oxide particle size also increased perhaps due to the extended calcination time for a portion of the Co. The particle size distributions after each adsorption step are given in Fig. 10. After 3rd adsorption, there is a broader distribution of particle sizes (45 ± 16) compared to after 1st adsorption (42 ± 10).

Table 4 summarizes the cobalt oxide particle size distribution of different carbons prepared by SEA with NaOH and NH_4OH. Monolayer deposition of Co oxides from the ammonical solutions is suggested by the lack of powder diffraction patterns. STEM analysis revealed that particles could be seen only after calcining the catalyst above 200 °C irrespective of whether NaOH or NH_4OH used to adjust the pH. The smallest particle size (and distribution) of 250 °C calcined samples was obtained with AS carbon using NaOH. Though nearly 21.1 wt% of Co can be loaded on CA carbon, particles obtained were not in a spherical shape, rather they formed small rod like structures with various (large) sizes. On TX particle size was 169 Å and on AS it was 50 Å. On VXC it was again aggregated in the form of (large) lumps. With NaOH, moderately small cobalt oxide particles are formed only on AS carbon where the metal loading is lowest.

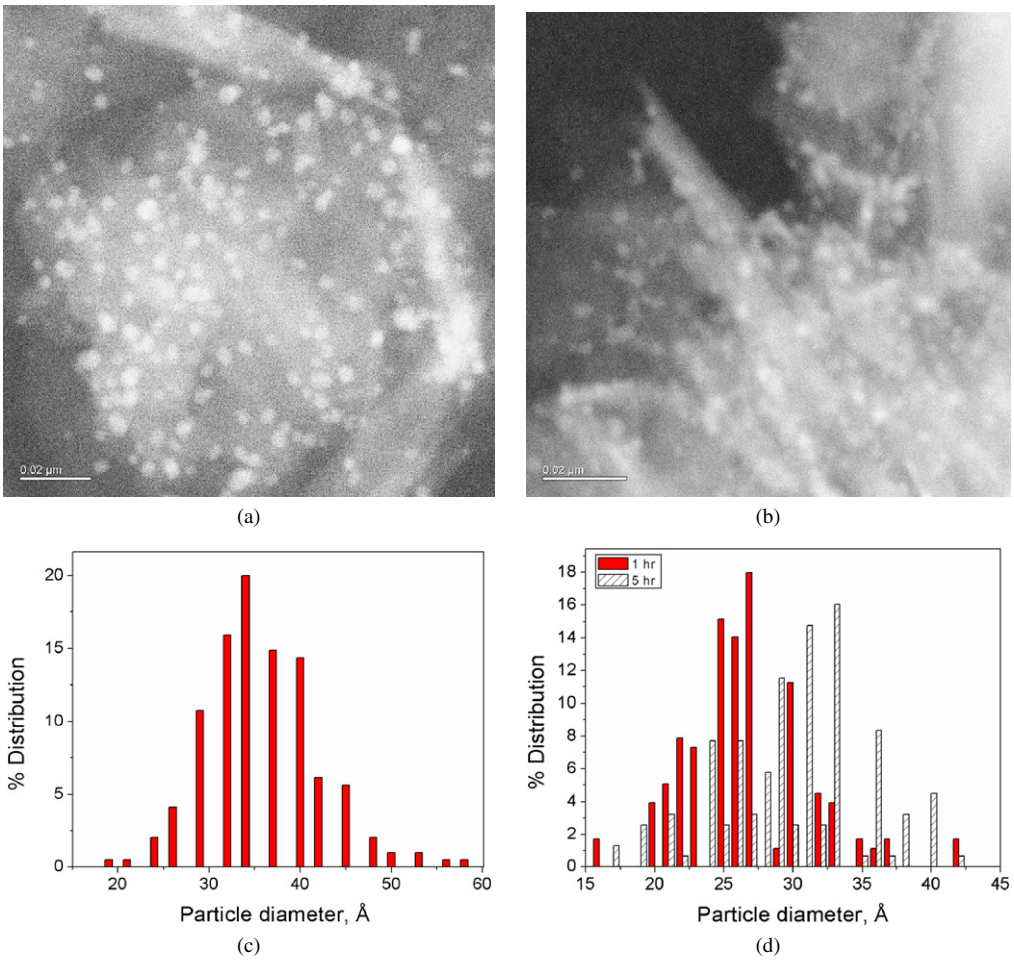

Fig. 9. STEM images of Co_3O_4 on (a) TX and (b) AS. (c) and (d) are particle size distribution of (a) and (b). NH_4OH was used to adjust the pH; pH_{final} was 10.3 and 10.1 for TX and AS, respectively.

For preparations using NH_4OH for the pH adjustments, generally, the cobalt loading is lower, but the particle size is smaller than those obtained with NaOH. The highest loading was again with CA carbon (6.7 wt%), but with spherical particles of around 33 Å. The lowest loading was obtained for AS at 1.5 wt% with particles of about 50 Å. Similarly, the oxide particle size on TX was about 50 Å with a loading of 4.0 wt% Co. The cobalt oxide on VXC carbon were large, aggregated lumps. While 50 Å cobalt oxide particles could be formed by the SEA method with NH_4OH on most carbon supports, under no conditions investigated did SEA lead to smaller cobalt oxide particles on VXC carbon. The reason for the difference with this carbon is not known.

Preparation by the IWI (incipient wetness impregnation) method using $Co(NO_3)_2$ yielded oxide particle sizes similar to that with SEA with NH_4OH and calcined at 250 °C, i.e., less than about 50 Å, even at high loadings of 20 wt%. X-ray diffraction studies revealed that cobalt particles possess Co_3O_4 crystalline phase on all types of carbon studied (typical XRD pattern of Co_3O_4/C was given in [1]). The smallest particles of 32 Å were obtained with BP followed by CA (36 Å), KB (37 Å), TX (42 Å) and KBB (72 Å). Like SEA with NaOH and NH_4OH, the particle size on VXC was large using the IWI method of preparation. Large particles were formed on AS carbon by IWI unlike the smaller particle by SEA. Based on the similarities in properties and preparations by SEA, AS carbon would be expected to give smaller cobalt oxide particles. The large size may results from the very high loading and the low surface area of AS carbon, i.e., surface density well over the monolayer limit.

IWI using CoHA is limited to low Co loadings due to the low solubility of CoHA. IWI of 1% Co on three carbons with differing PZC's were prepared by IWI of CoHA. As with the other preparations, the particle size on VXC were very large. Those on TX carbon were also large. This is in contrast to the 50 Å particles prepared by SEA of CoHA and NH_4OH, and two factors may be important. First, the pH of the IWI for a support with PZC of 4.5 will not have many negatively charged surface hydroxyl to strongly adsorb CoHA. In addition, the pH may also not be sufficient to affect the NH_3 ligand substitution reactions observed at higher pH. Thus, the structure of the adsorbed Co may be also very different. The latter has not been determined. The smallest oxide particle size (ca. 45 Å) was obtained with CA carbon. The PZC of CA carbon is 2.6, indicating that there is significant negative surface charge even in neutral impregnating solutions. This should result in a bet-

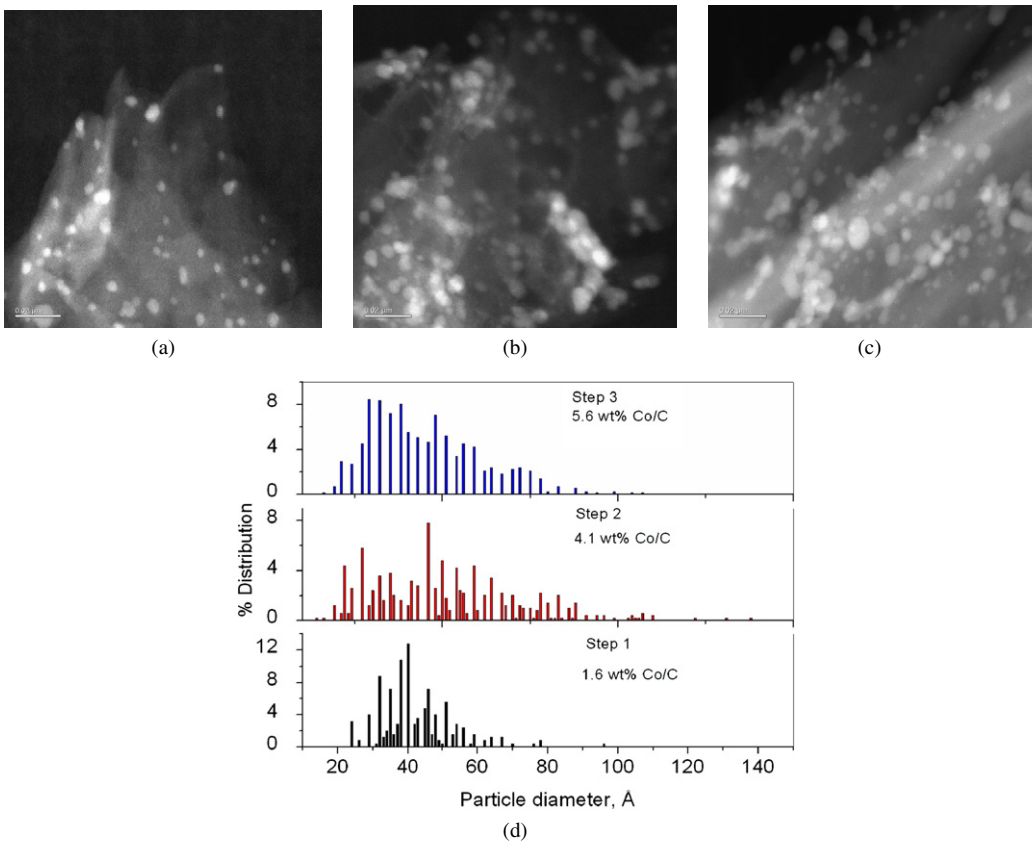

Fig. 10. STEM images and particles size distribution of cobalt oxides on TX carbon prepared with NH_4OH at an pH_{final} of ≈10.3 with multiple adsorption steps: (a) first, (b) second and (c) third adsorption procedure; (d) particle size distributions. Particle size and standard deviation in three steps are 42 ± 10 Å, 51 ± 21 Å and 45 ± 16 Å.

Table 4
Cobalt oxide particle size and standard deviation obtained on carbon supports, precursors, preparation methods and base (used for pH adjustment)

	Co/C (wt%)	Support	SA (m^2/g)	PZC	Precursor	Uptake (mol/m^2)	Particle diameter (Å)	
							x_N [a]	x_A [a]
SEA, NaOH	5.5	TX	280	4.5	CoHA	3.35E–06	169 ± 124	180 ± 130
	2.2	AS	115	5.2	CoHA	3.35E–06	50 ± 15	52 ± 17
	21.1	CA	1400	2.6	CoHA	3.25E–06	Small rod like structures	
	4.6	VXC	254	8.9	CoHA	3.23E–06	Aggregated lumps	
SEA, NH_4OH	4	TX	280	4.5	CoHA	2.50E–06	49 ± 15	50 ± 16
	1.5	AS	115	5.2	CoHA	2.30E–06	51 ± 12	51 ± 13
	6.7	CA	1400	2.6	CoHA	8.80E–07	33 ± 9	33 ± 12
	4	VXC	253	8.9	CoHA	2.70E–06	Aggregated lumps	
IWI	20	TX	280	4.5	$Co(NO_3)_2$	–	42 ± 20	45 ± 13
	20	KB	1250	9.4	$Co(NO_3)_2$	–	37 ± 12	42 ± 12
	20	BP	1475	9.5	$Co(NO_3)_2$	–	33 ± 6	33 ± 6
	20	CA	1400	2.6	$Co(NO_3)_2$	–	36 ± 15	43 ± 13
	20	KBB	1500	4.8	$Co(NO_3)_2$	–	72 ± 27	74 ± 30
	20	AS	115	5.2	$Co(NO_3)_2$	–	Aggregated lumps	
	20	VXC	254	8.9	$Co(NO_3)_2$	–	Aggregated lumps	
	1	TX	280	4.5	CoHA	–	483 ± 202	516 ± 184
	1	CA	1400	2.6	CoHA	–	45 ± 22	47 ± 16
	1	VXC	254	8.9	CoHA	–	187 ± 133	210 ± 97

SEA samples were prepared at pH of maximum uptake, i.e., pH_{final} ≈11.5 in NaOH, pH_{final} ≈10 in NH_4OH.
[a] x_N and x_A are number and surface area weighted mean particle sizes. Closeness of both values indicates homogeneity in size distribution. The error in metal uptake is ±5%.

ter support–cation interaction leading to smaller cobalt oxide particles.

4. Discussion

Consistent with the revised physical adsorption model, little CoHA is adsorbed at low pH and higher Co loadings are obtained at high pH on carbons with low PZC. At high pH, the surface is negatively charged due to deprotonation of the support hydroxyl groups and electrostatically attracts and adsorbs cations. Upon adsorption, CoHA undergoes a significant structural and electronic changes; and the metal uptake is more than one monolayer as expected by revised physical adsorption model. Therefore, the adsorption mechanism is postulated to be a *hybrid electrostatic–chemical* mechanism: electrostatic attraction of CoHA to the surface, and chemical interaction with the surface. This hybrid mechanism explains key experimental observations: the growth of even well dispersed oxide phases on the carbon surface and higher surface loadings than seen over silica (1.6 μmol/m^2), the exclusion of CoHA from the small pores of CA carbon (BJH adsorption average pore width = 48.4 Å) comes from the large size of the hydrated CoHA complex. The longest bond length between H atoms in trans position of $[Co(OH)_4]^{2-}$ is 4.631 Å. Even ten molecular clusters hinder their entry into the CA carbon pores.

For carbon with PZC 4.5, CoHA adsorbs at pH's greater than about 9, and XAS analysis indicates that the adsorbed Co has lost its NH_3 ligands and undergoes partial reduction. The functionality of semiquinone, pyridine-*N*-oxide groups [32] or the pi bonds in the aromatic rings give rise to the oxidation-reduction reaction wherein the metal complex is reduced and the carbon surface is oxidized. Carbon has been shown to reduce Pt^{4+} (chloride and oxychloride) complexes to Pt^{2+} at acidic conditions [33,34].

The structure of adsorbed CoHA appears to result from the interaction with the support surface, and the exact nature of the Co oxide species is also highly dependent on the adsorption pH. At a pH of about 9 on TX carbon, the adsorbed species are similar to small CoO particles. As the pH increases to about 10, the adsorbed species has a structure similar to Co_3O_4; while at higher pH the adsorbed species are likely Co^{2+} hydroxides. While adsorbed CoHA undergoes significant changes, even at a pH of 12 the non-adsorbed Co, i.e., the Co remaining in solution, is not reduced. The solution Co does undergo a ligand exchange, however, where one NH_3 is exchanged by Cl. This ligand exchange does not occur in the absence of the carbon support.

While the structure of the adsorbed Co changes with pH, so does reducibility of the cobalt oxide species. At 450 °C, Co_3O_4 is completely reduced, but the cobalt hydroxide complexes formed at pH greater than about 11 are only partially reduced. In order to obtain fully reduced, metallic Co, one needs to consider not only the support PZC, solution pH and metal complex charge, but also the structure of the adsorbed cobalt oxide. Adsorption of CoHA at a final pH around 10 is optimum and lower pH leads to little adsorption and higher pH gives species which are difficult to fully reduce.

For the SEA method of preparation, little CoHA would be expected to be adsorbed on supports with high PZC. For oxides with high PZC, for example alumina, there is little adsorption of cations, e.g., tetraamine platinum(II) at any pH [35]. However, the metal uptake on VXC (PZC = 8.9) is similar to that of low PZC carbons. Thus, for carbons, there is significant uptake of cationic complexes by supports with acidic, neutral or basic PZC's. One possibility could be, the hybrid process may also have a role in uptake over Vulcan; the surface can be oxidized as the CoHA is reduced, forming OH groups which can deprotonate and adsorb CoHA. These are not so prevalent as to firmly anchor the Co, however. Second possibility is the presence of both acidic and basic adsorption sites on carbons [36]. Previously, the carbons with acid and basic PZC's were reported to adsorb both cation and anion Pt complexes at pH's where the revised adsorption model would not expect significant adsorption [37]. The difference in adsorption on carbon compared to oxide supports was suggested to be due to the presence of multiple surface (hydroxyl) sites on carbon. The ratio of the acidic to basic hydroxyl groups determines the support PZC, but it appears that all carbons have some of each site. Thus, cations and anions may adsorb on carbon under conditions not expected from by the revised adsorption model for strong electrostatic adsorption.

The adsorption chemistry on carbon is also more complex than that on oxide supports (SiO_2, Al_2O_3, ZrO_2, etc.). For example on alumina, i.e., a support with high PZC, adsorbed anionic Au and Pt chloro-complexes have fewer Cl ligands (and more oxygen ligands, e.g., hydroxide or aquo) compared to solutions complexes [35,37]. The adsorbed Pt and Au complexes were consistent with a higher effective pH at the support surface compare to the impregnating solution. In addition, on silica, a support with low PZC, CoHA adsorbs at basic pH, but is not reduced or undergoes ligand exchange. CoHA ligand substitution is difficult in aqueous solutions, thus adsorbs unchanged on silica. The structural changes on oxides, therefore, can be understood by the effective pH of the support surface, while on carbon supports there can be changes in oxidation state and ligand substitution not expected from a change in the pH of the support.

The particle size of cobalt oxide formed by IWI of $Co(NO_3)_2$ is also different from that on oxide supports. On oxide supports, the resulting particle size is consistent with the Revised Adsorption model, i.e., strong metal–support interactions lead to smaller particles while poor interactions lead to larger particles. For example, at the weakly acidic pH of the impregnation solution, IWI of cationic Pt, $Pt(NH_3)_4^{2+}$ (or PtTA) on silica leads to larger particles, especially after calcination. With a PZC of about 4 and at a pH of 5, there is little surface charge and little PtTA is strongly adsorbed [5]. IWI of H_2PtCl_6, however, leads to small particles. With a PZC 9 and a pH of about 2 of the impregnating solution, the surface is positively charged and strongly attracts the anionic Pt [38].

From these considerations, one would expect that IWI of $Co(NO_3)_2$ on carbons with PZC from 2–5 would result in weak metal–support adsorption leading to large particles. One possible explanation is that the basic support groups, which appear

to be present even on carbons with low PZC, precipitate some cobalt. The resulting cobalt oxides/hydroxides have a high PZC, thus would strongly adsorb cationic Co. Whatever the explanation, IWI impregnation is an effective method for preparation of highly loaded catalysts with small particle size, at least when the surface density is not very high, i.e., several times monolayer coverage.

IWI of carbon with CoHA gives low metal loadings due the low solubility. The cobalt oxide particle size is generally consistent with electrostatic adsorption. Only in supports with low PZC is there sufficient negative surface charge to strongly adsorb the CoHA cations. For those supports, smaller particles result. For carbons with neutral to basic PZC's and weak adsorption, larger to very large particles form.

Control of the impregnation conditions to maximize the strong electrostatic attraction between the metal ions and the support lead to higher dispersions. In order to maintain the improved support coverage, it is also necessary to control the calcination temperature and time. Low temperature and short times appear preferred. In addition, for preparation of metallic particles, the reducibility of the supported Co is necessary and supported Co_3O_4 appears to be more thoroughly reduced than CoO and cobalt hydroxides. Since the nature of the supported cobalt oxide depends on the pH of adsorption solution, the optimum preparation conditions may not be at the pH that leads to highest metal loading. Rather the preferred preparation may be at the pH, which gives adsorbed species that are more easily reduced. For TX carbon using NH_4OH, complete reduction occurred on catalysts prepared at a pH of 10 which also is the pH required to obtain the highest Co loading. Preparations at higher and lower pH do not lead to complete reductions.

The results of this study demonstrate the importance of the optimization of the support surface charge for adsorption of the metal ions in catalyst preparation. In addition, upon adsorption the surface chemistry of carbon is more complex than that on other oxide supports (SiO_2, Al_2O_3, ZrO_2, etc.). In addition, with Co the nature of the adsorbed compounds strongly affects the reducibility and ultimately the formation of small metallic particles. For some carbons, e.g., VXC, no conditions have been found which give small particles. Since the latter is often used as a support in fuel cell applications, this remains an important support to develop an effective catalyst preparation method.

The reduction temperature obtained by TPR for different cobalt species does not match with that of XAS experiments. As per TPR results, the reduction of cobalt species takes place below 400 °C, but EXAFS show that catalysts prepared at pH_{final} 11.2 and 12.27 reduce partially to CoO and Co metal at 450 °C. The reason could be difference in partial pressure of H_2 used in TPR and XAS. In XAS experiments, reduction was carried out using 4% H_2 in Ar while in TPR 10% H_2 in Ar. It is well known that redox behavior of metal oxides strongly depends on the partial pressure of reductant/oxidant [39].

For the synthesis of bimetallics, it has been suggested [18] to apply the SEA method to supported oxides, such as supported cobalt oxide, and to direct the second metal onto that phase, both of which will reduce to bimetallics. The PZC of support and supported oxide should be well apart to execute selective adsorption of metal complex of second metal. For example, carbon support with PZC-4 and Co_3O_4 with PZC-9 would be suitable combination of two materials. Between pH 4–9 surface of carbon is negatively charged and that of Co_3O_4 is positively charged. A complex ion like $[PtCl_6]^{2-}$ can selectively adsorb on Co_3O_4 between pH 4–9. To this end, highly dispersed Co oxides on low PZC carbon are desired. We could not get well dispersed Co oxides with NaOH [1] but now with NH_4OH we've shown it's possible. The Co oxide phases in the dried samples are so well dispersed as to be invisible in STEM. With 250 °C calcination, they are still pretty small. IWI with Co nitrates also does well to form well dispersed Co_3O_4 and this may be a good, a very simple route for bimetallic catalyst preparation, although the Co oxide phase is not as well dispersed at SEA with no calcination.

Co nitrates normally form large particles when reduced [40], so while IWI with Co nitrates may be good for creating a semi-well dispersed Co oxide phase for bimetallics, it may not work so for creating small metallic Co particles. Sietsma et al. [41], have shown that calcining the Co/SiO_2 catalyst in an NO/He atmosphere prior to reduction leads to Co particles of size 4–5 nm when using $Co(NO_3)_2$ as a precursor. It may be possible to extend this treatment to carbon supports. With the use of hydrogen, however, the preliminary results from the XAS studies reveal that the reducibility and corresponding particle size of metallic particles depends on the precursor. To achieve small metallic Co particles in hydrogen, the idea is to prevent Co hydroxide formation.

5. Summary

In this study, we have demonstrated easy and efficient ways to prepare highly dispersed cobalt oxide and metallic cobalt on carbon catalysts using SEA of CoHA and IWI of $Co(NO_3)_2$. CoHA adsorbs on carbon supports at high pH and the amount is dependent on the pH and kind of alkali. The Co loading is higher using NaOH than NH_4OH. Although CoHA will adsorb on carbons at pH's not typically expected by the Revised Adsorption model, only under conditions consistent where strong electrostatic attraction, i.e., high solution pH giving a negatively charged support surface and metal cations, are small oxide particles obtained. IWI with $Co(NO_3)_2$ often gave small cobalt oxide particles even at high loadings, while small particles were obtained by IWI of CoHA on carbon with a acidic PZC (limited in metal loading <2% due to low solubility of CoHA in H_2O).

While 200 ppm CoHA (used in SEA preparations) was stable at basic pH, during the SEA catalyst preparation the adsorbed Co undergoes reductive deammination. The structure of the adsorbed Co is dependent on pH forming CoO (pH 9.2), Co_3O_4 (pH 9.8) and $Co(OH)_4^{2-}$ (pH > 11) in presence of NH_4OH. But in the presence of NaOH it transforms to Co_3O_4. Unlike the SEA preparation with NaOH where high Co loading are obtained at pH's greater than 12, with NH_4OH little Co is adsorbed. Although CoHA is stable at this pH, the non-adsorbed CoHA reacts to form $[Co^{+3}(NH_3)_5Cl]Cl_2$ in the presence of carbon support.

This study indicates that carbon supports significantly differ in the properties and ability to make small metal oxide or metallic particles. The complex nature of the functional surface groups leads to adsorption under conditions not expected by it's PZC and also affects complex chemical transformations, both reduction and ligand exchange.

Acknowledgments

The support of DOE/EERE (Hydrogen, Fuel Cells & Infrastructure Technologies Program) is gratefully acknowledged. Authors thank Mr. Ling Jiao, UIC for laboratory help and Dr. A.J. Kropf, Argonne National Laboratory for help with XAS experiments.

References

[1] L. D'Souza, L. Jiao, J.R. Regalbuto, J.T. Miller, A.J. Kropf, J. Catal. 248 (2007) 165.
[2] K.B. Agashe, J.R. Regalbuto, J. Colloid Interface Sci. 185 (1997) 174.
[3] J.R. Regalbuto, A. Navada, S. Shadid, M.L. Bricker, Q. Chen, J. Catal. 184 (1999) 335.
[4] M. Schreier, J.R. Regalbuto, J. Catal. 225 (2004) 190.
[5] J.T. Miller, M. Schreier, A.J. Kropf, J.R. Regalbuto, J. Catal. 225 (2004) 203.
[6] S. Özkar, R.G. Finke, J. Am. Chem. Soc. 124 (2002) 5796.
[7] M.S. Batista, E.I. Santiago, E.M. Assaf, E.A. Ticianelli, J. Power Sources 145 (2005) 50.
[8] M.M. Natile, A. Glisenti, Chem. Mater. 17 (2005) 3403.
[9] J. Mellor, R. Copperthwaite, N. Coville, Appl. Catal. A 164 (1997) 69.
[10] M.S. Batista, R.K.S. Santos, E.M. Assaf, J.M. Assaf, E.A. Ticianelli, J. Power Sources 134 (2004) 27.
[11] W.P. Ma, Y.J. Ding, L.W. Lin, Ind. Eng. Chem. Res. 43 (2004) 2391.
[12] T. Riedel, M. Claeys, H. Schulz, G. Schaub, S.S. Nam, K.W. Jun, M.J. Choi, G. Kishan, K.W. Lee, Appl. Catal. A 186 (1999) 201.
[13] S.V. Gredig, R.A. Koeppel, A. Baiker, Appl. Catal. A 162 (1997) 249.
[14] T. Joh, K. Doyama, K. Fujiwara, K. Maeshima, S. Takahashi, Organometallics 10 (1991) 508.
[15] R.G. Copperthwaite, F.M. Gottschalk, T. Sangiorgio, G.J. Hutchings, Appl. Catal. A 63 (1990) L11.
[16] G. Hutchings, F. Gottschalk, R. Hunter, S. Orchard, J. Chem. Soc. Faraday Trans. 85 (1989) 363.
[17] T. Halachev, V. Matveev, V. Idakiev, Y. Maksimov, A. Andreev, React. Kinet. Catal. Lett. 32 (1986) 257.
[18] J.R. Regalbuto, in: R.M. Richards (Ed.), Surface and Nanomolecular Catalysis, Taylor & Francis, 2006, p. 161.
[19] H. Bönnemann, W. Brijoux, R. Brinkmann, N. Matoussevitch, N. Waldöfner, N. Palina, H. Modrow, Inorg. Chim. Acta 350 (2003) 617.
[20] R.G. Finke, S. Özkar, Coord. Chem. Rev. 248 (2004) 135.
[21] O.F. Wohler, V. Sturm, E. Wege, H. von Kienle, M. Voll, P. Kleinschmit, in: W. Gerhartz (Ed.), Ullmann's Encyclopedia of Industrial Chemistry, vol. A5, VCH, Weinheim, 1986.
[22] W. Blyth, Chemical Economics Handbook: Graphite, SRI International, 1997.
[23] P. Roisson, J.P. Brundlle, P. Nortier, in: A.B. Stiles (Ed.), Catalyst Supports and Supported Catalysts: Theoretical and Applied Concepts, Butterworth, Boston, 1987, p. 11.
[24] J. Park, J.R. Regalbuto, J. Colloid Interface Sci. 175 (1995) 239.
[25] W.A. Spieker, J. Liu, J.T. Miller, A.J. Kropf, J.R. Regalbuto, Appl. Catal. A 232 (2002) 219.
[26] X. Hao, L. D'Souza, J.R. Regalbuto, Fundamental Study of Pt Impregnation of Carbon. 1. Adsorption Equilibrium and Kinetics, in preparation.
[27] X. Hao, L. Quach, J. Korah, W.A. Spieker, J.R. Regalbuto, J. Mol. Catal. A Chem. 219 (2004) 97.
[28] J.T. Miller, A.J. Kropf, Y. Zha, J.R. Regalbuto, L. Delannoy, C. Louis, E. Bus, J.A. van Bokhoven, J. Catal. 240 (2006) 222.
[29] G.L. Bezemer, P.B. Radstake, U. Falke, H. Oosterbeek, H. Kuipers, A. van Dillen, K.P. de Jong, J. Catal. 237 (2006) 152.
[30] F.B. Noronha, J. Perez Pena, M. Schmal, R. Fréty, Phys. Chem. Chem. Phys. 1 (1999) 2861.
[31] E. van Steen, G.S. Sewell, R.A. Makhothe, C. Micklethwaite, H. Manstein, M. de Lange, C.T. O'Connor, J. Catal. 162 (1996) 220.
[32] A. Montoya, O.J. Gil, F. Mondragon, N.T. Truong, Fuel Chem. Div. Prepr. 47 (2002) 424.
[33] H.E. Van Dam, H. Van Bekkum, J. Catal. 131 (1991) 335.
[34] X. Hao, On the Science of Catalyst Preparation: Platinum Impregnation over Carbon, Univ. of Illinois at Chicago, Chicago, 2004.
[35] W.A. Spieker, J.R. Regalbuto, Chem. Eng. Sci. 56 (2001) 3491.
[36] V. Strelko, D.J. Malik, M. Streat, Carbon 40 (2002) 95.
[37] J.R. Regalbuto, M. Schrier, X. Hao, W.A. Spieker, J.G. Kim, J.T. Miller, A.J. Kropf, Stud. Surf. Sci. Catal. 143 (2002) 45.
[38] W.A. Spieker, J. Liu, X. Hao, J.T. Miller, A.J. Kropf, J.R. Regalbuto, Appl. Catal. A 243 (2003) 53.
[39] M. Sturzenegger, L. D'Souza, R.P.W.J. Struis, S. Stucki, Fuel 85 (2006) 1599.
[40] Z.-J. Liu, Z. Xu, Z.-Y. Yuan, D. Lua, W. Chen, W. Zhou, Catal. Lett. 72 (2001) 203.
[41] J.R.A. Sietsma, J.D. Meeldijk, J.P. den Breejen, M. Versluijs-Helder, A. Jos van Dillen, P.E. de Jongh, K.P. de Jong, Angew. Chem. Int. Ed. Engl. 46 (2007) 4547.